VOLUME 118, NUMBER 50
DECEMBER 18, 1996

JOURNAL OF THE AMERICAN CHEMICAL SOCIETY

Redox-Triggered Secondary Structure Changes in the Aggregated States of a Designed Methionine-Rich Peptide

Heather L. Schenck, Gregory P. Dado, and Samuel H. Gellman*

Contribution from the Department of Chemistry, University of Wisconsin, Madison, Wisconsin 53706

Received June 17, 1996[⊗]

Abstract: We have previously shown that methionine can be used as a "switchable" residue for the design of peptides with alternative secondary structure preferences in the aggregated state (*J. Am. Chem. Soc.* **1993**, *115*, 12609). Redox-induced secondary structure changes in the 18-residue peptide Ac-YLKAMLEAMAKLMAKLMA-NH_2 result from conversion of lipophilic methionine (M) to hydrophilic methionine sulfoxide (M°), which transforms a peptide capable of adopting an amphiphilic α-helical conformation into a peptide capable of adopting an amphiphilic β-strand conformation. Here we present a detailed characterization of the third oxidation state of this peptide, in which the methionine residues are oxidized to the sulfone state. The sulfone form behaves similarly to the sulfoxide form, even though the sulfone group is somewhat less hydrophilic than the sulfoxide group. These results provide support for the concept that the conformational preferences of peptides and proteins are strongly dependent upon the linear ordering of hydrophilic and lipophilic residues ("amphiphilic order").

The way in which a protein's one-dimensional arrangement of amino acid residues specifies the three-dimensional structure of the native state is still unclear.[1] Protein design efforts should help to elucidate the mysterious relationship between sequence and conformation, because design goals are not necessarily limited to the goals that natural selection has imposed on the evolution of biological proteins. In trying to expand the repertoire of protein behaviors beyond those recognized in the biological realm, the protein designer is forced to probe the operational linkage between sequence and folding pattern.

We recently described a strategy for generating proteins that could alter their global folding patterns, from predominantly α-helical secondary structure to predominantly β-sheet secondary structure, in response to an external stimulus.[2] Such a profound structural alteration might allow one to turn a protein's function on and off. Our strategy requires a "switchable" residue that can be interconverted between hydrophilic and lipophilic forms. Methionine was employed as the switchable residue, since this residue is lipophilic,[3] but methionine sulfoxide, which can be generated reversibly, is expected to be hydrophilic. The 18-mer Ac-YLKAMLEAMAKLMAKLMA-NH_2 (**1**) was shown to form α-helices in the aggregated state, while the tetrasulfoxide derivative (**1**°) was shown to form β-sheets in the aggregated state.[2] The redox-dependent behavior of aggregated forms of **1**/**1**° suggests that it may be possible to use switchable residues to drive coupled changes in the secondary and tertiary structures of larger designed polypeptides. Indeed, Vogt et al.[4] have shown that methionine oxidation activates the fifth component of human complement, C5, a process that is believed to require significant structural rearrangement of the protein. García-Echeverría[5] has recently reported that an α-helical coiled-coil dimer can be disrupted by oxidation of a methionine residue at the lipophilic interface.[6]

The dramatic effect of side chain oxidation in peptide **1**[2] provides insight into the extent to which a protein's three-dimensional folding pattern is dictated by the one-dimensional

[⊗] Abstract published in *Advance ACS Abstracts*, December 1, 1996.
(1) Dill, K. A. *Biochemistry* **1990**, *29*, 7133.
(2) Dado, G. P.; Gellman, S. H. *J. Am. Chem. Soc.* **1993**, *115*, 12609.
(3) Radzicka, A.; Wolfenden, R. *Biochemistry* **1988**, *27*, 1664.
(4) Vogt, W. *Free Radicals Biol. Med.* **1995**, *18*, 93.
(5) García-Echeverría, C. *Bioorg. Med. Chem. Lett.* **1996**, *6*, 229.

S0002-7863(96)02026-4 CCC: $12.00

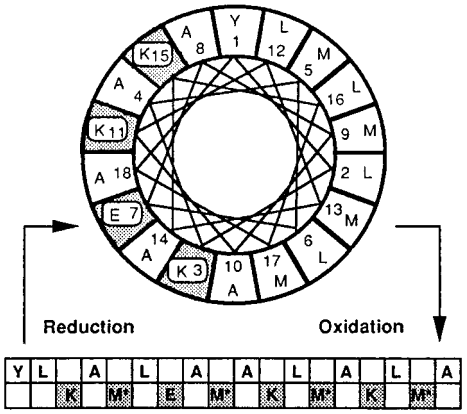

Figure 1. Schematic depiction of peptide **1** in the α-helical state (upper) and peptide **1**° in the β-strand state (lower). These depictions highlight the well-defined polar and nonpolar surfaces displayed by each redox state in the secondary structure illustrated (polar residues are stippled). (A = alanine, E = glutamic acid, K = lysine, L = leucine, M = methionine, M* = methionine sulfoxide or sulfone, and Y = tyrosine.)

ordering of hydrophilic and lipophilic residues ("amphiphilic order"). Water-soluble proteins, in the native state, tend to display hydrophilic residues on their solvent-exposed surfaces and to bury lipophilic residues in their dehydrated cores.[7] This simple trend has served as the basis for most protein design efforts to date.[8] These efforts have focused on the creation of amphiphilic sheets and/or helices (i.e., extended secondary structures in which hydrophilic residues are displayed on one well-defined surface and lipophilic residues are displayed on another well-defined surface), with the intent that tertiary structure will result from hydrophobically driven burial of lipophilic surfaces against one another. Figure 1 illustrates how side chain oxidation/reduction in peptide **1** alters amphiphilic order and thereby induces conformational switching: **1** can form an amphiphilic α-helix, with methionine residues as constituents of the lipophilic surface, while **1**° can form an amphiphilic β-strand, with the methionine sulfoxide residues contributing to the hydrophilic surface.

Early exploration of conformational control via amphiphilic order involved synthetic peptides that could adopt amphiphilic β-strands. Brack and Orgel observed that the alternating copolymer poly(Val-Lys) forms β-sheet aggregates in aqueous solutions containing salt.[9] In the extended conformation of poly(Val-Lys), the valine side chains project from one side of the main chain and the lysine side chains from the other. Brack and Orgel attributed the β-sheet aggregation to hydrophobically driven association of surfaces defined by the valine side chains. Kaiser and co-workers recognized the amphiphilic order-based design that nature has employed for peptide toxins (e.g., melittin), hormones (e.g., β-endorphin and gonadatropin-releasing hormone), and lipoprotein particles.[10] In these systems, relatively short segments (15−20 residues) can form amphiphilic α-helices. This secondary structure is particularly stable at hydrophilic/lipophilic interfaces, e.g., membrane surfaces or the air−water interface. Like the strictly alternating copolymers examined by Brack and Orgel,[9] amphiphilic helix-forming peptides can provide their own interfacial environment: adoption of the amphiphilic secondary structure is cooperatively enhanced by peptide aggregation. DeGrado et al. have shown that the self-association of peptides displaying amphiphilic secondary structures can serve as a model system for tertiary structure formation in larger designed polypeptides.[8a,11]

Amphiphilic order is not the only determinant of tertiary structural stability. Polypeptides designed on this principle, or isolated from combinatorial libraries constructed on this principle, have tended not to display the highly specific and kinetically stable conformations that characterize most natural globular proteins.[8d,12] This situation may result from a lack of detailed complementarity among interacting side chains on adjacent secondary structural elements. Indeed, among peptides designed to adopt α-helical coiled-coil structures, the oligomerization state has been shown to depend critically on a small number of interhelical side chain−side chain contacts.[13]

In addition to side chain interactions (or lack thereof), conflicts with the intrinsic conformational preferences of individual residues could undermine protein design guided by amphiphilic order. Valine and isoleucine, for example, are among the most hydrophobic residues, but because their side chains are branched at the β-position, these residues display an intrinsic preference for β-sheet conformations.[14] One way to probe the relative importance of amphiphilic order and the intrinsic conformational preferences of individual residues is to construct sequences in which the residue conformational preferences conflict with the secondary structure specified by amphiphilic order. For copolymers containing only lysine and leucine, both of which have high intrinsic preferences for α-helical states but lower preferences for β-sheet states. Brack and Spach showed that the secondary structure adopted in the aggregated state depends strongly on sequence.[15] Strict leucine/lysine alternation led to β-sheet formation, in the presence of salt, while polymers with more random residue distribution had a greater tendency toward α-helix formation. DeGrado and Lear examined leucine/lysine-containing oligomers of defined length and sequence, observing stark secondary structural differences between strict residue alternation (β-sheet) and a more complex sequence intended to promote amphiphilic α-helix formation.[16] Xiong et al. have recently extended this approach by showing that sequences containing multiple β-branched residues will aggregate in α-helical form, as dictated by amphiphilic order, despite intrinsic residue preferences for β-sheet formation.[17] These findings were presaged by the striking discovery that the pulmonary surfactant-associated polypeptide SP-C adopts a highly α-helical conformation in solution, even though nearly half of the helical residues are valine or isoleucine.[18]

The behavior of polylysine provides further evidence for the

(6) For photochemically driven conformational changes, see: (a) Ulysse, L.; Cubillos, J.; Chmielewski, J. *J. Am. Chem. Soc.* **1995**, *117*, 8446. (b) Willner, I.; Rubin, S. *Angew. Chem., Int. Ed. Engl.* **1996**, *35*, 367 and references therein.

(7) Creighton, T. E. *Proteins: Structures and Molecular Properties*, 2nd ed.; New York: Freeman, 1993.

(8) (a) DeGrado, W. F. *Adv. Protein Chem.* **1988**, *39*, 51. (b) Mutter, M.; Vuilleumier, S. *Angew. Chem., Int. Ed. Engl.* **1989**, *28*, 535. (c) Cohen, C.; Parry, D. A. D. *Proteins*: *Struct., Funct., Genet.* **1990**, *7*, 1. (d) Betz, S. F.; Raleigh, D. P.; DeGrado, W. F. *Curr. Opin. Struct. Biol.* **1993**, *3*, 601. (e) Kametar, S.; Schiffer, J. M.; Xiong, H.; Babik, J.; Hecht, M. H. *Science* **1993**, *262*, 1680.

(9) Brack, A.; Orgel, L. E. *Nature* **1975**, *256*, 383.

(10) Kaiser, E. T. *Acc. Chem. Res.* **1989**, *22*, 47.

(11) Regan, L.; DeGrado, W. F. *Science* **1988**, *241*, 976.

(12) Davidson, A. R.; Lumb, K. J.; Sauer, R. T. *Nat. Struct. Biol.* **1995**, *2*, 856.

(13) Harbury, P. B.; Zhang, T.; Kim, P. S.; Alber, T. *Science* **1993**, *262*, 1401.

(14) (a) Chou, P. Y.; Fasman, G. D. *Adv. Enzymol.* **1978**, *47*, 45. (b) Kim, C. A.; Berg, J. M. *Nature* **1993**, *362*, 267. (c) Minor, D. L.; Kim, P. S. *Nature* **1994**, *367*, 660. (d) Minor, D. L.; Kim, P. S. *Nature* **1994**, *371*, 264. (e) Smith, C. K.; Withka, J. M.; Regan, L. *Biochemistry* **1994**, *33*, 5510.

(15) Brack, A.; Spach, G. *J. Am. Chem. Soc.* **1981**, *103*, 6319.

(16) DeGrado, W. F.; Lear, J. D. *J. Am. Chem. Soc.* **1985**, *107*, 7684.

(17) Xiong, H.; Buckwalter, B. L.; Shieh, H.-M.; Hecht, M. H. *Proc. Natl. Acad. Sci. U.S.A.* **1995**, *92*, 6349.

(18) Johansson, J.; Szyperski, T.; Curstedt, T.; Wüthrich, K. *Biochemistry* **1994**, *33*, 6015.

importance of amphiphilic order.[19] This polymer can adopt α-helical, β-sheet, or random coil conformations, depending on the pH and sample history. The origins of these conformational preferences have not been elucidated, but it seems likely that the changing preferences are related to variations in the proportion and pattern of protonated side chains. Mutter et al. have shown that short synthetic peptides can also undergo pH-dependent conformational changes in the aggregated state,[20] although, as for polylysine, the structural basis for this switching is unclear.[21]

The profound effect of side chain oxidation on the secondary structural preferences of aggregated **1** and **1**° constitutes strong evidence that amphiphilic order overrides the intrinsic conformational preferences of the residues employed.[2] In this system, unlike those described in the preceding paragraph, amphiphilic order does not depend upon acid−base equilibria, and the rationale for alternative secondary structure preferences in different oxidation states is clear (Figure 1). Side chain oxidation should have little effect on the intrinsic conformational preference of the residue, since the oxidation site is three atoms out from the main chain. Here we extend our examination of this system by describing the methionine sulfone-containing peptide Ac-YLKAM°°LEAM°°AKLM°°AKLM°°A-NH_2 (**1**°°; M°° = methionine sulfone).[22] This more highly oxidized peptide behaves similarly to sulfoxide **1**°. We chose the sulfone for detailed studies because **1**° is likely to be a mixture of diastereomers, by virtue of the stereogenicity of the sulfoxide sulfur atom, while there is no possibility of stereoisomerism with sulfone **1**°°.

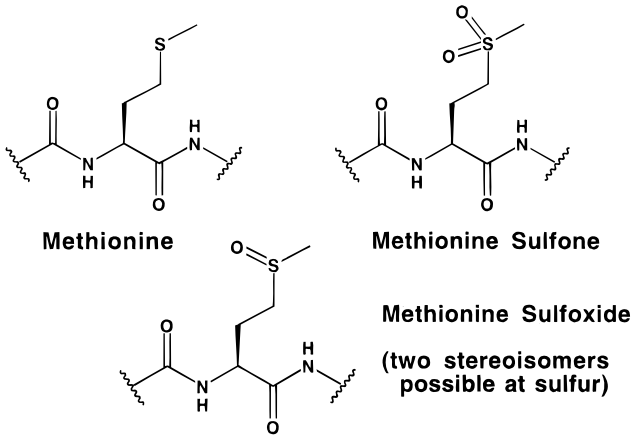

Results and Discussion

Residue Polarity. The polarity change that results from oxidation of the methionine side chain to either sulfoxide or sulfone was evaluated by examining the partitioning of amino acid derivatives between aqueous and nonpolar solutions.

(19) Davidson, B.; Fasman, G. D. *Biochemistry* **1967**, *6*, 1616.

(20) Mutter, M.; Gassmann, R.; Buttkus, U.; Altmann, K.-H. *Angew. Chem., Int. Ed. Engl.* **1991**, *30*, 1514.

(21) In discussing the pH-dependent interconversion of α-helical and β-sheet forms, Mutter et al. comment "what exactly determines the preference for one or the other type of secondary structure under different sets of experimental conditions remains elusive". This uncertainty stems from the fact that the amphiphilic order of the sequences employed in ref 20 is designed to allow formation of *both an amphiphilic α-helix and an amphiphilic β-sheet simultaneously.* In contrast, our 18-mer sequence is designed to allow an amphiphilic α-helix (but not an amphiphilic β-sheet) in the reduced form, and an amphiphilic β-sheet (but not an amphiphilic α-helix) in the oxidized forms.

(22) For methionine sulfone in proteins, see: (a) Dolla, A.; Florens, L.; Bianco, P.; Haladjian, J.; Voodrouw, G.; Forest, E.; Wall, J.; Guerlesquin, F.; Bruschi, M. *J. Biol. Chem.* **1994**, *269*, 6340. (b) Buzy, A.; Bracchi, V.; Sterjiades, R.; Chroboczek, F.; Thibault, P.; Gagnon, J.; Jouve, H. M.; Hudry-Clergeon, G. *J. Protein Chem.* **1995**, *14*, 59.

Table 1. Residue Polarity[a]

amino acid[b]	P_m[c]	$\Delta G°$ (kcal/mol)[d]
norleucine	0.018 ± 0.002	2.38 ± 0.07
leucine	0.027 ± 0.002	2.14 ± 0.05
methionine	0.046 ± 0.002	1.82 ± 0.02
alanine	0.8 ± 0.1	0.1 ± 0.1
methionine sulfone	1.9 ± 0.2	−0.3 ± 0.2
glycine	2.1 ± 0.1	−0.44 ± 0.03
threonine	2.3 ± 0.2	−0.49 ± 0.05
serine	10.8 ± 0.5	−1.41 ± 0.03
methionine sulfoxide[e]	11 ± 3	−1.4 ± 0.2
glutamine	78 ± 3	−2.57 ± 0.02

[a] Residue polarity assessed by the method described in the text, involving partitioning of amino acid derivatives between water and methylene chloride. [b] Amino acid derivatives **2** were used. [c] The partition coefficient between water and methylene chloride, $[\mathbf{2}]_{water}/[\mathbf{2}]_{methylene\ chloride}$; the uncertainty is $\pm 2\sigma$ for multiple determinations. [d] Free energy of partitioning corresponding to the partition coefficient P_m, according to the equation $\Delta G° = -RT \ln(P_m)$; the uncertainty is $\pm 2\sigma$ for multiple determinations. [e] Examined as a diastereomeric mixture.

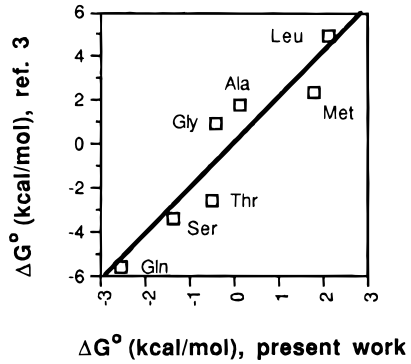

Figure 2. Comparison of free energies of transfer ($\Delta G°$) for amino acid derivatives **2** between water and methylene chloride, as determined in the present study, and $\Delta G°$ values reported for side chain model compounds partitioned between water and cyclohexane (ref 3). The line represents the best linear fit to the data and corresponds to the equation $y = 0.0464 + 2.09x$ (correlation coefficient 0.868).

Amino acid derivatives **2** were prepared by standard methods,

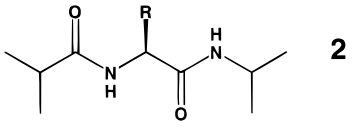

and their partitioning between CH_2Cl_2 and H_2O was monitored by IR spectroscopy, using the strong amide I absorbance to determine concentration in each layer. Table 1 shows the results of these studies, in terms of the partition coefficient, P_m (eq 1), and $\Delta G°$ for transfer from CH_2Cl_2-saturated H_2O to H_2O-saturated CH_2Cl_2 (eq 2). (Equation 1 assumes equal volumes

$$P_m = [\mathbf{2}]_{water}/[\mathbf{2}]_{mec} \quad (1)$$

$$\Delta G° = -RT \ln(P_m) \quad (2)$$

of the two solvents; details of the partitioning experiments are provided in the Experimental Section.) Figure 2 shows that there is a good linear correlation between the $\Delta G°$ values determined by our method and the $\Delta G°$ values reported by Radzicka and Wolfenden[3] for partitioning of side chain model compounds between cyclohexane and H_2O, for the seven residues leucine, methionine, alanine, glycine, threonine, serine, and glutamine.

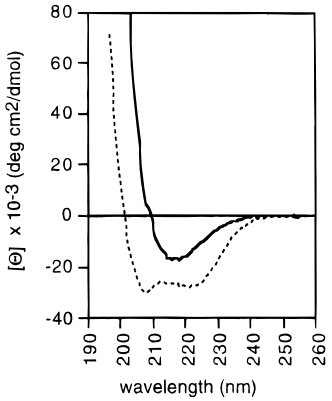

Figure 3. Circular dichroism of peptides **1** (0.88 mM; lower curve) and **1**°° (0.12 mM) in H_2O at room temperature. For **1**, the minima occur at 208.5 nm ($-30\,400$ deg cm^2 dmol^{-1}) and 221 nm ($-28\,200$ deg cm^2 dmol^{-1}); for **1**°°, the minimum occurs at 218 ($-17\,500$ deg cm^2 dmol^{-1}). The sample of **1**°° was equilibrated for 118 h prior to analysis.

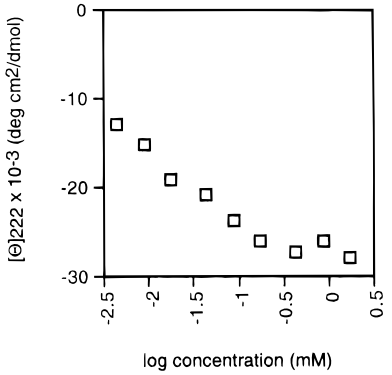

Figure 4. $[\theta]_{222}$ for peptide **1** as a function of the logarithm of peptide concentration in H_2O.

The data in Table 1 indicate that methionine is lipophilic, in accord with the conventional view.[3] Methionine sulfoxide, on the other hand, is quite hydrophilic, nearly equivalent to serine. Thus, as anticipated, interconversion between methionine and methionine sulfoxide constitutes a profound alternation of residue polarity. Among small molecules, sulfones are moderately less polar than the analogous sulfoxides, and this trend is observed in Table 1. Despite the decrease in polarity relative to the sulfoxide, methionine sulfone is still modestly hydrophilic.

Circular Dichroism: Effects of Peptide Concentration on Secondary Structure. Figure 3 compares far-UV CD data for **1** and **1**°° in aqueous solution. Circular dichroism in this region arises largely from the backbone amide groups and is commonly used to evaluate peptide secondary structure.[23] The data for **1** indicate that this peptide is largely α-helical (minima at ca. 208 and 221 nm), while the data for **1**°° indicate extensive β-sheet formation (minimum at ca. 218 nm).

The extent of α-helix formation, as monitored by the ellipticity at 222 nm, is dependent upon the concentration of **1** (Figure 4). As the peptide concentration rises from 0.0044 to 1.76 mM, the ellipticity at 222 nm becomes more negative, but there is little change above 0.2 mM. This behavior suggests that α-helix formation is stabilized by peptide self-association, as expected on the basis of the fact that **1** can form an amphiphilic α-helix[10,11] and the general observation that monomeric α-helices are never more than marginally stable in peptides of this length. The extent of α-helix formation in other short peptides has been estimated on the basis of the limiting

(23) Johnson, W. C. *Proteins*: *Struct., Funct., Genet.* **1990**, *7*, 205.

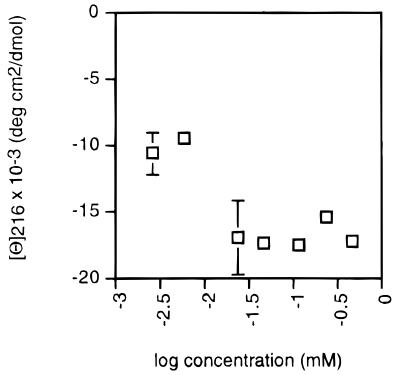

Figure 5. $[\theta]_{216}$ for peptide **1**°° as a function of the logarithm of peptide concentration in H_2O. Samples were prepared from a 0.63 mM stock solution of **1**°°. The samples at the two highest concentrations were equilibrated for 51 h prior to analysis, and the samples at the lower concentrations were equilibrated for 312 h (in each case, equilibrium appeared to have been reached).

$[\theta]_{222}$ values observed in TFE titrations.[24] TFE titration with **1** indicates $-28\,200$ deg cm^2 dmol^{-1} as a limiting value for maximum α-helix formation (extrapolated to pure water), which suggests that the $[\theta]_{222}$ of $-26\,700$ deg cm^2 dmol^{-1} observed for **1** in aqueous solution at ≥ 0.2 mM corresponds to ca. 95% α-helix formation.

Figure 5 shows the effect of the concentration of **1**°° on the ellipticity at 216 nm, i.e., near the minimum that is characteristic of β-sheet formation. At concentrations ≥ 0.023 mM, $[\theta]_{216}$ remains constant at approximately $-17\,000$ deg cm^2 dmol^{-1}. Polylysine in the β-sheet form displays a $[\theta]_{216}$ of ca. $-18\,000$ deg cm^2 dmol^{-1},[25] and the value observed for **1**°° therefore suggests extensive β-sheet formation, ≥ 0.023 mM. For the two data points at lowest concentration (0.0057 and 0.0026 mM), $[\theta]_{216}$ is significantly lower, ca. 10 000 deg cm^2 dmol^{-1}. This diminution of the β-sheet signal in the most dilute samples suggests that β-sheet formation requires self-assocation of **1**°°.

Analytical ultracentrifugation[26] (data not shown) provided direct evidence that **1**°° aggregates in solution. Sedimentation velocity experiments at 25 000 rpm indicated the presence of monomer as well as a variety of species much larger than monomeric **1**°°, and sedimentation equilibrium experiments at 2000 rpm suggested a mean aggregate molecular weight of approximately 10^6.

Infrared Spectroscopy: Slow Secondary Structural Changes for the Sulfone Peptide. Figure 6 compares amide I region IR data for **1** and **1**°° in aqueous solution. Data from the amide I region are particularly useful for distinguishing antiparallel β-sheets from other secondary structures.[27] The major band at 1620 cm^{-1} and the minor band at 1695 cm^{-1} observed for **1**°° constitute strong evidence that this peptide exists largely in the β-sheet form under these conditions. (The amide I band splitting arises from transition dipole coupling that is characteristic of the spatial arrangement of amide groups found in antiparallel sheets.[27a]) The lack of significant absorbance in the region 1650−1670 cm^{-1} for **1**°° indicates that there is little random coil or α-helical secondary structure in this sample. For **1**, the major amide I band occurs at 1651 cm^{-1}, which is consistent with either an α-helix or a random coil.[27] Although amide I

(24) Lyu, P. C.; Wang, P. C.; Liff, M. I.; Kallenbach, N. R. *J. Am. Chem. Soc.* **1991**, *113*, 3568.

(25) (a) Sarkar, P. K.; Doty, P. *Proc. Natl. Acad. Sci. U.S.A.* **1966**, *55*, 981. (b) Greenfield, N.; Fasman, G. D. *Biochemistry* **1969**, *8*, 4108.

(26) Hansen, J. C.; Lebowitz, J.; Demeler, B. *Biochemistry* **1994**, *33*, 13155 and references therein.

(27) (a) Krimm, S.; Bandekar, J. *Adv. Protein Chem.* **1986**, *38*, 181. (b) Dong, A.; Huang, P.; Caughey, W. S. *Biochemistry* **1990**, *29*, 3302.

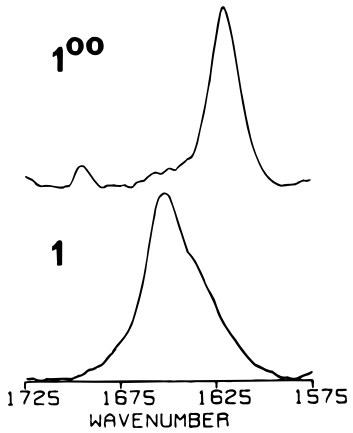

Figure 6. Amide I IR data for peptides **1** (1.8 mM; maximum at 1651 cm^{-1}) and **1**°° (1.9 mM; maxima at 1695 and 1620 cm^{-1}) in H_2O at room temperature (the latter solution was allowed to equilibrate for 20 h prior to analysis). Data were obtained using a circular internal reflectance cell with a ZnSe crystal. The spectra have been base-line-corrected.

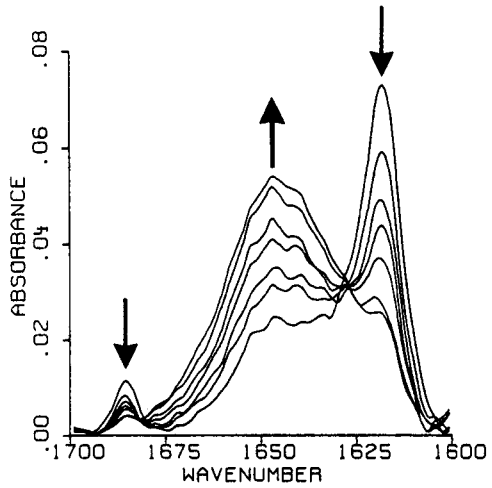

Figure 7. Time course of changes induced upon addition of TFE to a D_2O solution of **1**°°, as monitored by amide I′ IR data. (These experiments began with a solution of 2.1 mM **1**°° in D_2O that had been equilibrated for 48 h. This stock solution was diluted with D_2O and then TFE, to give a final TFE proportion of 11 mol % and a final peptide concentration of 0.45 mM.) Overlaid spectra were obtained at 1 min, 12 s (1:12), 2:18, 3:17, 5:15, 8:15, 36:32, and 120:15 after the TFE addition. All spectra have been base-line-corrected.

region data do not reliably distinguish between these two conformational states, the CD data in Figures 3 and 4 show that **1** exists largely as an α-helix rather than a random coil under these conditions.

Addition of TFE converts the *β*-sheet adopted by **1**°° in pure aqueous solution to an α-helix (Figures 7 and 8). This solvent-induced conformational change is not surprising, since it is well-established that TFE strongly promotes helical conformations.[24] It is surprising, however, that this conformational change is slow. The relatively long time period required for complete conversion to an α-helix (from several minutes to several hours, depending on the proportion of TFE) presumably results from the fact that *β*-sheet formation in aqueous solution requires aggregation; disentangling this *β*-sheet aggregate must involve a substantial kinetic barrier.

Figure 7 shows the time course of the amide I′ changes induced by adding TFE (11 mol % final concentration) to a D_2O solution of **1**°°. (The solvent switch from H_2O to D_2O produces small shifts in amide I bands, because this vibrational

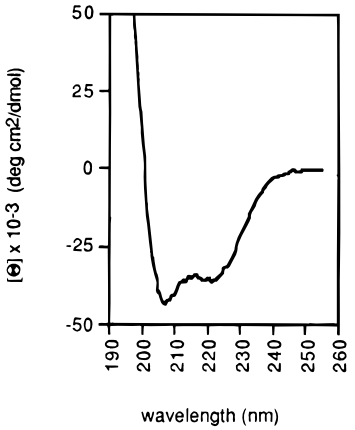

Figure 8. Circular dichroism of peptide **1**°° (0.053 mM) in 12 mol % TFE in H_2O, after 6 h of equilibration.

mode has an N−H/D bend component.[27] Bands observed in D_2O are conventionally designated with a prime, i.e., amide I′.) Conformational interconversions between a *β*-sheet and an α-helix are very conveniently monitored by changes in the amide I region of the IR spectrum, since the IR features characteristic of a *β*-sheet are much better resolved from the α-helix (and random coil) features than is true for CD spectroscopy. In the spectrum obtained ca. 1 min after the addition of TFE (Figure 7), the dominant band at 1618 cm^{-1} and the smaller band at 1685 cm^{-1} indicate that the peptide is still largely in the *β*-sheet form. At this point, however, there is also a significant increase in absorbance around 1650 cm^{-1}, relative to **1**°° in pure D_2O. By 30 min, the broad absorbance at 1646 cm^{-1} is dominant, and only minor amounts of the *β*-sheet bands remain. CD data obtained after a water−TFE solution of **1**°° has achieved equilibrium show a classical α-helix signature (Figure 8).

Assembly of the *β*-sheet aggregate of **1**°° in aqueous solution is also a slow process. Figure 9 shows the time-dependent changes that occur in the amide I′ region upon dissolution of **1**°° in D_2O. Figure 9a shows the solid-state IR spectrum (KBr pellet) of the peptide before dissolution. This spectrum suggests that the peptide is conformationally heterogeneous: the band at 1631 cm^{-1} indicates partial *β*-sheet formation, but the major amide I band at 1657 cm^{-1} implies that most of the peptide is not in the *β*-sheet form. Figure 9b shows the IR spectrum obtained 70 s after dissolution in D_2O. The major band in the amide I′ region, 1618 cm^{-1}, suggests that most of the peptide has adopted the *β*-sheet form, a conclusion that is supported by the appearence of a small band at 1684 cm^{-1}. The peptide is still heterogeneous at this point, however, as indicated by the significant shoulder around 1650 cm^{-1}. Figure 9c shows that this shoulder has disappeared after 60 min, and that the sample is now a pure *β*-sheet. Figure 9d shows the evolution of the FT-IR data between 70 s and 60 min. Slow formation of a *β*-sheet upon dissolution of **1**°° in water was observed with several other samples of the peptide, but there was considerable variation in the time required for complete *β*-sheet formation, from several minutes to several hours, among samples.

Slow disruption of the *β*-sheet aggregate of **1**°° in aqueous solution, upon dissolution, can be detected by CD spectroscopy. Figure 10 shows a plot of $[\theta]_{216}$ as a function of time upon dilution of a 0.63 mM sample at **1**°° to 0.0057 mM (aqueous solution). The sample required >4 days to achieve equilibrium, with CD suggesting the equilibrium state to be only partially a *β*-sheet. The CD data shown in Figure 5 were obtained with samples generated by serial dilution of a 0.63 mM sample of **1**°°; all solutions were allowed to come to equilibrium before the CD data were obtained.

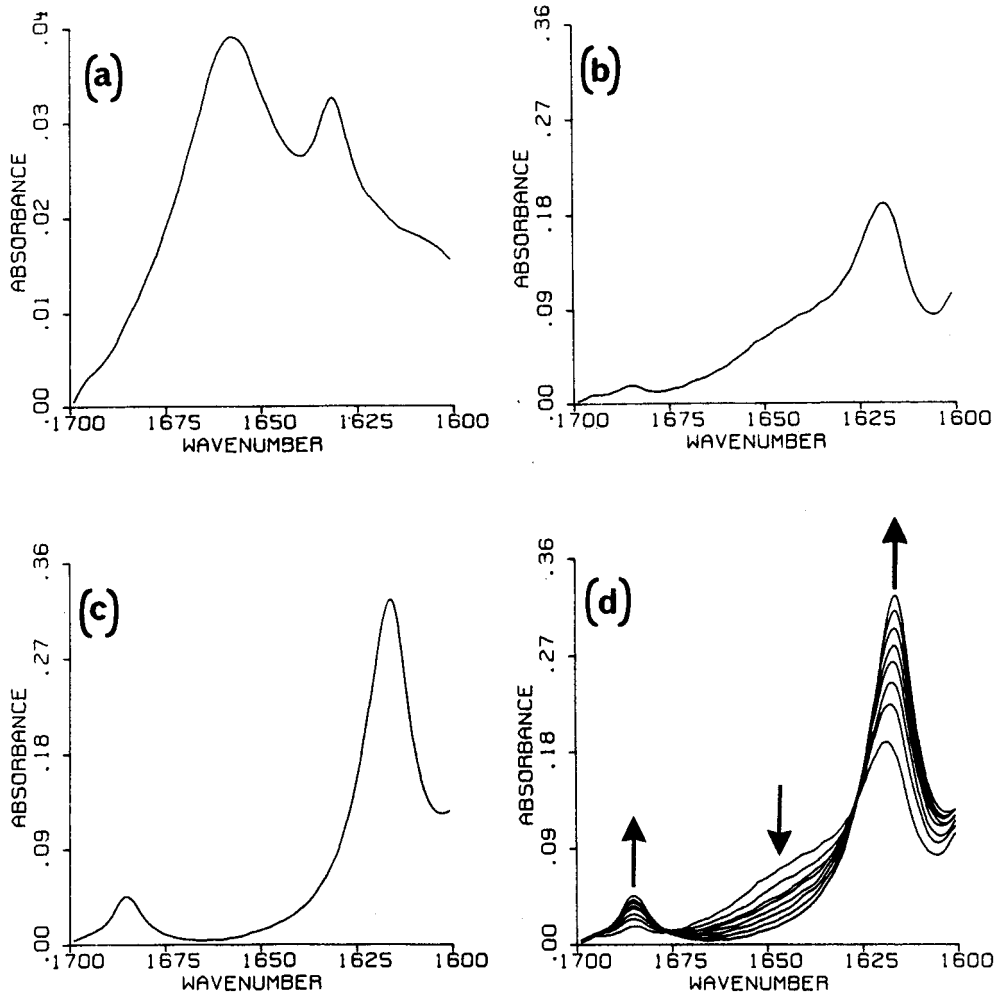

Figure 9. Time course of changes induced by dissolution of **1**°° in D_2O (1.64 mM). All spectra have been base-line-corrected. (a) Solid state IR spectrum (KBr pellet) of the sample of **1**°° used to obtain the solution data, *before* dissolution. (b) IR spectrum from 1 min, 10 s (1:10) in the time course. (c) IR spectrum from 60:00 in the time course. (d) Overlaid spectra obtained at 1:10, 2:10, 3:05, 4:00, 5:00, 7:00, 12:00, and 60:00 (from top to bottom at 1650 cm^{-1}) after dissolution.

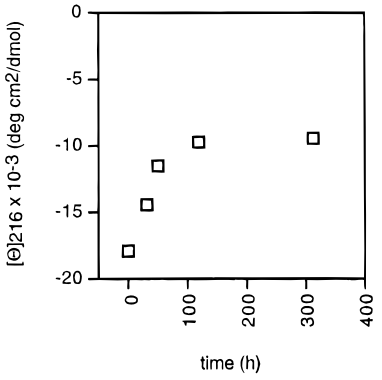

Figure 10. Time course of changes in $[\theta]_{216}$ for peptide **1**°° after dilution of a 0.63 mM aqueous solution to 0.0057 mM (the final concentration corresponds to the second lowest concentration in Figure 5).

Conclusions

1. Amphiphilic Order as a Determinant of Protein Structure. Sulfone peptide **1**°° behaves similarly to the previously reported sulfoxide version **1**° in that both form antiparallel β-sheet aggregates in water. This conformational preference stands in contrast to the propensity of reduced peptide **1** to form α-helical aggregates. The fact that this dramatic secondary structural difference can be induced by conversion of just 4 of the 18 side chains from lipophilic to hydrophilic provides support for the notion that amphiphilic order is a strong determinant of protein folding patterns.

2. Kinetics and Thermodynamics of β-Sheet Stability. The β-sheet aggregate formed by **1**°° in pure water appears to be very stable thermodynamically, since the peptide appears to be fully self-associated even at 0.023 mM. This stability is manifested also in the difficulty of disassembling the β-sheet aggregate. TFE-induced conversion of this β-sheet aggregate to the α-helical form requires hours to go to completion, and the partial β-sheet disruption resulting from dilution of an aqueous solution to <0.01 mM requires days, implying that there is a substantial kinetic barrier to pulling the β-strands apart. There is a significant kinetic barrier to assembly of the β-sheet aggregate as well, as indicated by the time period required for complete β-sheet formation when **1**°° is dissolved in water.

Experimental Section

Materials. Chemicals were obtained from Aldrich except where noted, and used without further purification unless specified. Fmoc-amino acid pentafluorophenyl esters, RapidAmide resin cartridges, 1,3-diisopropylcarbodiimide, and 1,2-ethanedithiol were obtained from Dupont. Acetic anhydride, DMF, and HPLC grade acetonitrile were obtained from EM Science. Water for HPLC was obtained from a Millipore filtration system. *N*,*N*-Dimethylformamide was distilled under high vacuum at <30 °C from ninhydrin. HPLC solvents were filtered through a 0.45 μm nylon filter. IR spectra were obtained at room temperature on a Nicolet 740 FTIR spectrometer, using either a

transmission cell with CaF_2 windows (150 μm path length) or a horizontal attenuated total reflectance apparatus with a ZnSe crystal. Each IR spectrum was ratioed against a background spectrum, and a spectrum of pure solvent was subtracted from each sample spectrum where appropriate. CD spectra were obtained on an OLIS/Cary 60 CD spectrophotometer at room temperature, 1.5 nm bandwidth, 0.5 nm resolution, 4 scans/sample, path length 0.01−10 mm. LSIMS mass spectra were recorded on a VG Autospec M mass spectrometer using 3-nitrobenzyl alcohol as a matrix, resolution 2000−2500.

Peptide Synthesis. Peptides were prepared using standard solid phase techniques with N^{α}-Fmoc-protected amino acid pentafluorophenyl esters on RapidAmide resin (0.1 mmol resin cartridges, Dupont), which provides C-terminal peptide amides on cleavage. The tyrosine side chain was protected as the *tert*-butyl ether, and the glutamic acid side chain was protected as the *tert*-butyl ester. The lysine side chains were Boc protected. Couplings were performed on the RaMPS solid phase peptide synthesizer (Dupont) using the standard protocol of 2.5 equiv of amino acid and 1 equiv of HOBT (hydroxybenzotriazole hydrate) in DMF; failed couplings were repeated using either HOBT in DMF or 2.5 equiv of 1,3-diisopropylcarbodiimide and HOBT in 1:1 CH_2Cl_2−DMF. The extent of couplings was monitored using the Kaiser ninhydrin test. The N-terminal Fmoc was removed by treatment for 9−11 min with 1:1 piperidine−DMF. Acetylation of the N-terminal ends of completed peptides was accomplished using 5.7 equiv of *N*,*N*-diisopropylethylamine and 21 equiv of acetic anhydride in DMF. Side chain deprotection and cleavage of peptide from the resin were accomplished by stirring the resin with 3 mL of trifluoroacetic acid (TFA), 120 μL of water-liquefied phenol, and 15 μL of 1,2-ethanedithiol in a 10 mL flask for 16 h. The resin was filtered and rinsed with TFA, and the TFA mixture was concentrated to 1−2 mL under a stream of N_2. The residue was taken up in 25 mL of diethyl ether and centrifuged for 3 min; the ether was decanted, and the procedure was repeated three times. After two additional rinses of the solid peptide with 1.5:1 ethyl acetate−diethyl ether, the peptide was dissolved in a minimum amount of water and lyophilized. Tripeptides were purified by semipreparative reversed-phase HPLC on a Jones C18 column with a linear gradient of 2−10% acetonitrile in water and constant 0.1% TFA. Octadecapeptides were subjected to reducing conditions prior to purification:[28] 20 mg of crude peptide dissolved in 4 mL of 2.9 M aqueous β-mercaptoethanol was heated at 90 °C for 1 h, followed by a diethyl ether wash and lyophilization. Octadecapeptides were purified on a semipreparative Vydac C4 column using a linear gradient of 55−58.5% acetonitrile in water with constant 0.2% HFBA (heptafluorobutyric acid). Solutions were concentrated by rotary evaporation and lyophilized to yield white solids, the purities of which were confirmed by analytical reversed-phase HPLC (>90%).

For purified octadecapeptides, the heptafluorobutyrate counterions were exchanged for acetate by applying a solution of peptide (2.5−8 mg) in 4:1 15 mM aqueous AcOH−CH_3CN to a column of strong anion exchange resin (AG1-X8; acetate form; BioRad) and eluting with 4:1 15 mM aqueous AcOH−CH_3CN. Exchange was confirmed by ^{19}F NMR (absence of signals from heptafluorobutyrate).

Sulfone oxidation of peptides was undertaken using acid-washed glassware. Performic acid (1.95 mL of formic acid, 49 μL of 30% H_2O_2) was preformed at room temperature for 2 h, at which time the performic acid solution and the peptide, dissolved in 250 μL of formic acid and 50 μL of methanol, were chilled individually in an ice−water bath for 0.5 h. Then, 50 equiv of performic acid was added to the peptide solution at 4 °C, and the reaction was maintained on ice for 7.5 h or until completion, as judged by HPLC (an aliquot of the reaction containing 0.05 mg of peptide was quenched into an excess of aqueous β-mercaptoethanol and injected onto an analytical C4 HPLC column, using a linear gradient of 28−40% acetonitrile [0.2% HFBA] over 15 min, and then isocratic 40% acetonitrile for an additional 15 min, for octadecapeptides).[29] The reaction was worked up when approximately 90% of the sample was seen to elute as the tetrasulfone, as confirmed by mass spectral analysis. The remaining 10% of the sample was seen eluting just prior to the main fraction, and was believed to be trisulfone−monosulfoxide, on the basis of mass spectral evidence and HPLC profiles of the oxidation process. Stopping the reaction at 90% completion prevented formation of products that eluted after the main fraction and appeared to be overoxidized; these overoxidation products were never characterized. Contamination of the tetrasulfone sample with the trisulfone−monosulfoxide impurity was expected to have no significant effect on the sample behavior, as the tetrasulfoxide peptide also forms a β-sheet structure.[2] The reaction was worked up by dilution into 12 mL of H_2O and lyophilization.[29]

Octadecapeptide concentrations were determined by tyrosine absorbance at 275 nm, from which the baseline absorbance at 300 nm had been subjected, using an extinction coefficient of 1450.[30] A small aliquot of peptide solution was diluted with 8 M guanidine hydrochloride and water to yield 600 μL of 6 M guanidine hydrochloride−peptide solution, which was allowed to stand at room temperature for 1−4 h prior to analysis by UV.

Mass Spectrometry of Peptides. Ac-Tyr-Leu-Lys-Ala-Met-Leu-Glu-Ala-Met-Ala-Lys-Leu-Met-Ala-Lys-Leu-Met-Ala-NH_2. LRMS (LSIMS) for $C_{93}H_{162}N_{22}O_{22}S_4$ (**1**), calcd 2068.7, obsd 2069.1. LRMS for $C_{93}H_{162}N_{22}O_{30}S_4$ (**1**°°), calcd 2196.7, obsd 2197.3.

Amino Acid Analysis. Peptide **1** was subjected to amino acid analysis by hydrolysis, phenyl isocyanate (PITC) derivatization, and HPLC analysis.[31] A 0.5 mg sample of **1** was hydrolyzed with 1 mL of 6 N HCl at 110−130 °C for 24 h, after which the solvent was removed under high vacuum. The hydrolyzate was reacted for 10 min with PITC in a solution of 10:5:2:3 acetonitrile−pyridine−triethylamine−water. Solvents and excess PITC were completely removed under high vacuum, and the residue was analyzed by reversed-phase HPLC, monitoring at 254 nm. Relative amounts of constituent amino acids were determined by integration of the (phenylthiocarbamoyl)amino acid (PTC-amino acid) peaks, the retention times of which were determined by analysis of PTC-amino acid standards. All amino acids were assumed to have equal integrated response factors, except for lysine, which was assumed to have an integrated response factor twice that of other derivatives. Amino acids were quantified relative to PTC-alanine.

residue	expected	PITC	residue	expected	PITC
alanine	5.0	5.0	lysine	3.0	2.8
glutamic acid	1.0	0.92	methionine	4.0	3.8
leucine	4.0	4.3	tyrosine	1.0	1.1

Diamide Partitioning Studies. Partitioning studies have been performed using water-saturated dichloromethane solutions of diamide derivatives **2**, partitioning into dichloromethane-saturated water. Experiments were conducted at room temperature; aqueous solutions were not buffered. Generally, equal volumes of dichloromethane and water were used, except in cases where a solute showed a strong preference for one phase. In these cases, the proportion of unfavorable to favorable phase was increased to 2−5:1, and correction for the volume difference was made in calculation (eq 3). Phases were mixed in a rocking tray

$$P_m = (A_{unpart} - A_{part})/(A_{part})(\text{vol of } CH_2Cl_2/\text{vol of } H_2O) \quad (3)$$

for 1−2 h, and the resulting emulsion was allowed to separate prior to IR analysis. A solvent spectrum of water-saturated dichloromethane was subtracted from sample spectra, with further correction of water subtraction as needed (using a subtraction of two dichloromethane solutions containing different amounts of water). Spectra were baseline-corrected. Subtraction of baseline-corrected amide I peaks provided P_m values, which were used to calculate the free energy of transfer between phases (eq 2). The concentration dependence of partitioning behavior was checked for several diamides by comparing partition data for initial diamide concentrations of 2, 10, and 20 mM; in all cases, no concentration dependence was seen.

Diamide Synthesis. Amino acid derivatives **2** were prepared by standard methods. Details are given here for the methionine, methionine sulfoxide, and methionine sulfone versions. Syntheses of the other derivatives are described elsewhere.[32]

***N*-(*tert*-Butyloxycarbonyl)methionine *N*′-Isopropylamide.** To a solution of 2.49 g (10 mmol) of *N*-(*tert*-butyloxycarbonyl)methionine

(28) Freilinger, A. F.; Zull, J. E. *J. Biol. Chem.* **1984**, *259*, 5507.
(29) Hirs, C. H. W. *J. Biol. Chem.* **1956**, *219*, 611.
(30) (a) Marqusee, S.; Robbins, V. H.; Baldwin, R. L. *Proc. Natl. Acad. Sci. U.S.A.* **1989**, *86*, 5286. (b) Brandts, J. F.; Kaplan, L. J. *Biochemistry* **1973**, *12*, 2011.
(31) Heinrikson, R. L.; Meredith, S. C. *Anal. Biochem.* **1984**, *136*, 65.
(32) Dado, G. P. Ph.D. Thesis, University of Wisconsin−Madison, 1993.

in 75 mL of THF was added 1.725 g (15 mmol) of *N*-hydroxysuccinimide and 2.575 g (12.5 mmol) of 1,3-dicyclohexylcarbodiimide; a white precipitate quickly formed. The reaction mixture was stirred under N_2 for 1 h and was then cooled to 0 °C in an ice bath. Isopropylamine (2.55 mL, 30 mmol) was added, and the reaction mixture was stirred under N_2 at room temperature for 18 h. The precipitate was then removed by gravity filtration, and the filtrate was concentrated to a white solid. The crude product was purified by SiO_2 column chromatography eluting with 50% EtOAc in hexane to afford the desired amide as a white solid in 83% yield: mp 100−101 °C; ^{1}H NMR ($CDCl_3$) δ 6.07 (br d, 1 H, NH), 5.20 (br d, 1 H, NH), 4.22−3.95 (m, 3 H, NH*CH*$_2$CO, NH*CH*$(CH_3)_2$), 2.59−2.45 (m, 2 H, SCH_2), 2.10 (s, 3 H, SCH_3), 2.07−1.84 (m, 2 H, CH_2), 1.43 (s, 9 H, $(CH_3)_3$C), 1.14 (d, 6 H, CH(*CH*$_3$)$_2$); IR (CH_2Cl_2) 3424 (NH), 3339 (NH), 1708 (carbamate C═O), 1673 (amide I), 1497 (amide II) cm^{-1}; EI MS *m*/*e* 234.1032, calcd for $C_9H_{18}N_2O_3S$ ($M^+ - C_4H_8$) 234.1038.

***N*$^\alpha$-Isobutyrylmethionine *N*′-Isopropylamide.** To 1.74 g (6 mmol) of *N*-(*tert*-butyloxycarbonyl)methionine *N*′-isopropylamide was added 2.5 mL of 4 N HCl in dioxane. After the solution had been stirred under N_2 for 1 h, N_2 gas was bubbled through the solution for 20 min and the dioxane was then removed by rotary evaporation. The resulting viscous syrup was dried briefly in vacuo and then dissolved in 30 mL of THF. To this solution was added 2.5 mL of triethylamine; a white precipitate immediately formed. The reaction mixture was cooled to 0 °C in an ice bath, and 0.94 mL of isobutyryl chloride was added. After the reaction mixture had been stirred under N_2 at room temperature for 1 h, the precipitate was removed by gravity filtration and washed with several portions of THF. However, this precipitate contained much of the desired product, so the solid was recombined with the filtrate. After concentration of this mixture, the crude product was purified by SiO_2 column chromatography eluting with 3% MeOH in $CHCl_3$, followed by recrystallization from dichloroethane to afford the desired amide as a white crystalline solid in 70% yield: mp 204.5−206.5 °C; ^{1}H NMR ($CDCl_3$) δ 6.33 (br, 1 H, NH), 6.22 (br, 1 H, NH), 4.52 (q, 1 H, NH*CH*CO), 4.09−3.99 (m, 1 H, NH*CH*$(CH_3)_2$), 2.70−2.50 (m, 2 H, SCH_2), 2.39 (sep, 1 H, CO*CH*$(CH_3)_2$), 2.12 (s, 3 H, SCH_3), 2.06−1.93 (m, 2 H, CH_2), 1.16 (d, 6 H, CH(*CH*$_3$)$_2$); IR (0.001 M in CH_2Cl_2) 3423 (NH), 3330 (NH), 1671 (amide I), 1665 (amide I), 1524 (amide II), 1501 (amide II) cm^{-1}; EI MS *m*/*e* 260.1561, calcd for $C_{12}H_{24}N_2O_2S$ 260.1558.

***N*$^\alpha$-Isobutyrylmethionine Sulfoxide *N*′-Isopropylamide.** To a solution of 0.13 g (0.5 mmol) of *N*$^\alpha$-isobutyrylmethionine *N*′-isopropylamide in 3.0 mL of CH_2Cl_2 and 3.0 mL of HOAc at 0 °C was added 60 μL (0.6 mmol) of 30% aqueous H_2O_2.[28] After the reaction mixture had been stirred at room temperature for 4 h, the solvents were removed by vacuum rotary evaporation. The crude product was purified by SiO_2 column chromatography eluting with 2−5% MeOH in $CHCl_3$ to afford the desired sulfoxide as a white solid in 96% yield: mp 202.5−203 °C; ^{1}H NMR ($CDCl_3$, 1:1 mixture of diastereomers) δ 7.06, 7.04, 6.92 (3 br d, 2H, NH), 4.61, 4.58 (2 q, 1 H, NH*CH*CO), 4.10−3.90 (m, 1 H, NH*CH*$(CH_3)_2$), 3.0−2.2 (overlapping m, 5 H, *CH*$(CH_3)_2$, SCH_2, CH_2), 2.67, 2.58 (2 s, 3 H, SCH_3), 1.17−1.12 (m, 12 H, 2 CH(*CH*$_3$)$_2$); IR (0.001 M in CH_2Cl_2) 3420 (NH), 3261 (NH), 1664 (amide I), 1522 (amide II), 1500 (amide II) cm^{-1}; EI MS *m*/*e* 277.1581, calcd for $C_{12}H_{25}N_2O_3S$ ($M^+ + H$) 277.1586.

***N*$^\alpha$-Isobutyrylmethionine Sulfone *N*′-Isopropylamide.** To 0.13 g (0.5 mmol) of *N*$^\alpha$-isobutyrylmethionine sulfoxide *N*′-isopropylamide in 3.0 mL of CH_2Cl_2 and 3.0 mL of formic acid at 0 °C was added 150 μL (1.5 mmol) of 30% aqueous H_2O_2.[29] After the reaction mixture had been stirred at room temperature for 18 h, the solvents were removed by vacuum rotary evaporation, and the white solid residue was dried *in vacuo*. The crude product exhibited a single spot by analytical SiO_2 TLC (15% MeOH in $CHCl_3$). This material was passed through a SiO_2 chromatography column, eluting with 3% MeOH in $CHCl_3$, to afford the desired sulfone as a white solid in quantitative yield: mp 207.5−208.5 °C; ^{1}H NMR ($CDCl_3$) δ 6.62 (br, 2 H, 2 NH), 4.60 (q, 1 H, NH*CH*CO), 4.05−3.95 (m, 1 H, NH*CH*$(CH_3)_2$), 3.30−3.00 (m, 2 H, SCH_2), 2.99 (s, 3 H, SCH_3), 2.43 (sep, 1 H, CO*CH*$(CH_3)_2$), 2.28−2.18 (m, 2 H, CH_2), 1.18−1.12 (m, 12 H, 2 CH(*CH*$_3$)$_2$); IR (0.001 M in CH_2Cl_2) 3420 (NH), 3350 (NH), 1667 (amide I), 1524 (amide II), 1496 (amide II) cm^{-1}; EI MS *m*/*e* 293.1540, calcd for $C_{12}H_{25}N_2O_4S$ ($M^+ + H$) 293.1535.

Acknowledgment. This research was supported by the Army Research Office. We thank Dr. Darryl McCaslin for assistance with the analytical ultracentrifuge studies. We thank Professor C. Sih and Mr. G. Girdaukas for access to and assistance with the CD spectropolarimeter in the School of Pharmacy of the University of Wisconsin−Madison, and Ms. Carol MacHarg and Mr. Paul Kostel of Vydac/The Separations Group for helpful advice. H.L.S. and G.P.D. were supported in part by National Research Service Awards (Grant T32 GM08932) from the National Institute of General Medical Sciences.

JA962026P